

# Serious Microsats Need Serious Instruments, MIBS and the First Results

J. Leijtens, B. de Goeij, E. van der Meché, M. Eschen, and A. Court

**Abstract** To go beyond the point where micro satellites are seen as a way to qualify technology for use on a “real” satellite, small instruments are needed that can perform a socially or scientifically significant task. MIBS is a spectrometer operating in the thermal infrared wavelength region, designed in the frame of the phase A study for the ESA EarthCARE mission, which uses an uncooled 2D microbolometer array detector instead of the more common MCT detectors, which allows for a significant reduction in size, and power consumption. Although the detectivity of microbolometers is less than for MCT detectors, they offer specific advantages due to the wider wavelength response, which can be tailored to suit the application. This allows the design of an instrument that can image both the 3 . . . 5 and 8 . . . 12 micron bands simultaneously, and which can be seen as an instrument that can be used to assist in weather prediction during everyday use (its original goal) and in addition be used for forest fire detection and monitoring. In order to demonstrate feasibility of the concept a breadboard has been designed and built of which the first measurement results are presented here.

## 1 Introduction

The microbolometer spectrometer is a prism spectrometer that uses a combination of reflective optics and a high speed camera in order to obtain an as high as possible NETD. (Fig. 1)

---

J. Leijtens

TNO science and Industry, Stieltjesweg 1, 2628 CK Delft  
e-mail: johan.leijtens@tno.nl

B. de Goeij

TNO science and Industry, Stieltjesweg 1, 2628 CK Delft

E. van der Meché

TNO science and Industry, Stieltjesweg 1, 2628 CK Delft

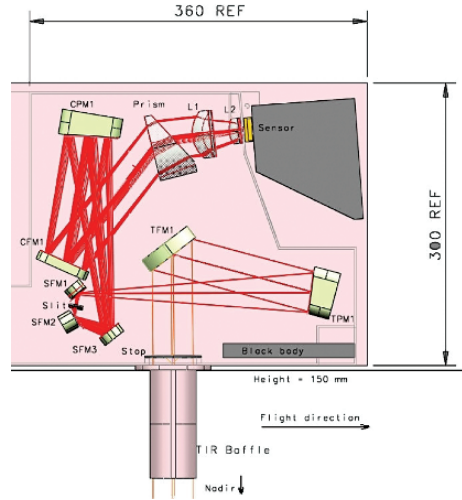
M. Eschen

TNO science and Industry, Stieltjesweg 1, 2628 CK Delft

A. Court

TNO science and Industry, Stieltjesweg 1, 2628 CK Delft

**Fig. 1** Principle optical diagram of MIBS



The nadir view is looking down in this picture, and the incoming radiation is deflected by TFM1 to the collimator TPM1 which focuses on the slit via compensation mirror SFM1. The slit image is again formed into a collimated beam via compensation mirror SFM2, foldmirror SFM3, collimation mirror CFM1 and foldmirror CFM1. The radiation is then dispersed by the prism and imaged on the detector via Germanium lenses L1 and L2. TFM1 is the calibration mirror which is used to point at either one of two blackbody's incorporated in the design or the scene. For this purpose the mirror of the MIBS breadboard can be rotated by means of a small stepper motor.

Given the close proximity of the parts CFM1, SFM1, slit and SFM2 (and the desire to assemble the entire system on basis of manufacturing tolerances as much as possible) a single mechanical assembly is created out of these parts. This so called slit assembly (Fig. 2) is used as the starting point of the alignment procedure.

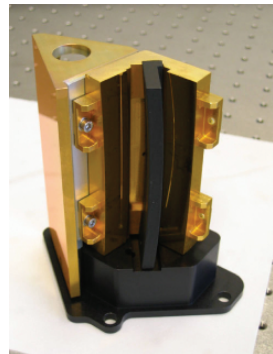
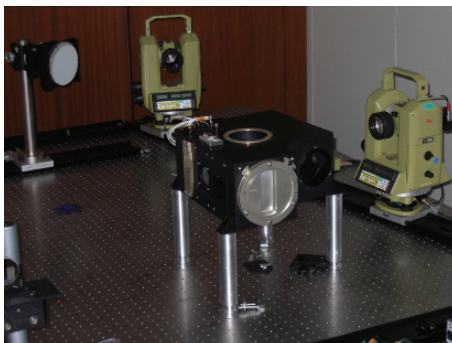


**Fig. 2** Slit assembly

**Fig. 3** Alignment setup



Subsequent mounting of SFM3 and CPM1 completes the installation of the collimating branch. Mounting of TPM1 and TFM1 completes the telescope branch. The alignment of the optical parts is facilitated through the availability of wedged shims that allow to adjust the tilts of the components in an easy way and a number of dedicated alignment openings are provided in the housing in order to be able to measure the position of the optical components.

Since the entire system up to the prism is reflective (with a transmissive slit) all of the measurements can be done using standard theodolites. During the assembly and alignment of the system it was proven that the alignment philosophy worked well in the sense that although additional shimming possibilities were provided, they were not needed during the alignment and all parts are mounted using manufacturing tolerances and dedicated alignment shims only.

The camera assembly consists of the mount for the prism and the camera lenses. It is a selfstanding assembly which is made of titanium in stead of the aluminium which is the base material for the rest of the instrument. (Fig. 4). Untill now no further measurements have been made on this assembly with exception of the mounting position of the prism.

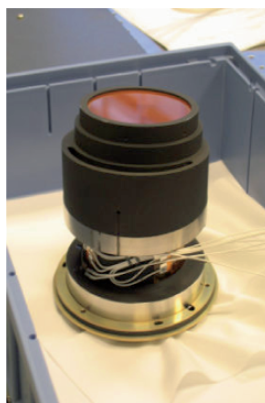


**Fig. 4** Camera assembly ready for mounting

The camera assembly has dedicated heaters and temperature sensors in order to enable accurate temperature stabilization. This stabilization is required in case absolute temperature measurements are to be made with the instrument. The need to stabilize the temperature is related to the absorption in the Germanium. Since the absorption in the Germanium is less for lower temperatures, and the change in absolute radiation is less for lower temperatures, there is a preference to operate the optical bench at as low as possible temperatures in order to have an as high as possible absolute radiometric accuracy.

## 2 Current Status

The MIBS breadboard has been assembled and is ready for the measurement and verification phase (Fig. 5). Since the setup has only been used to do NETD measurements, the thermal control hardware has been mounted but has not yet been operated.

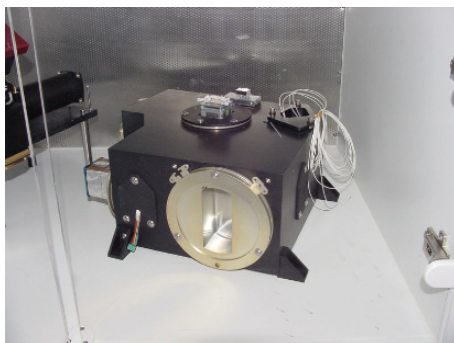


**Fig. 5** MIBS in space incubator

## 3 Measurements Performed

Since the obtainable NETD is inherently lower when comparing a filter based instrument and a spectrometer, and absolute radiometric accuracy may be easier to obtain with a spectrometer, the prime focus for the measurements performed were optical alignment and NETD.

### 3.1 Optical Measurements

The optical alignment went very well with the exception of mounting of the prism. The rotation of the prism in its holder is slightly above spec (1,3 mrad instead of 1 mrad) which will potentially influence the co-registration for the end of swath. This however is not considered to be a serious deviation and is left as is for the

moment. In case full performance is required in a later stage, this mis-alignment can be solved through a more elaborate alignment procedure, but for the moment it is deemed more important to know what the deviation from nominal is, then to be within the nominal tolerances as there are no real fixed requirements for the breadboard and recalculation (with the actual values) will allow the correlation of real life measurements with theoretical predictions.

As for the other optical tolerances everything else with exception of the nadir pointing repeatability has been proven to be well within spec. The nominal optical axis is positioned at  $90 \pm 0.001$  degrees with respect to the front face of the instrument well within the 0.1 mrad requirement. The repeatability of the stepper-motor used to rotate the calibration mirror however has been proven to be within 0.08 degrees, the 0.08 degrees repeatability is less then required (0.14 mrad against 0.1 mrad required) but this is not seen as a serious issue at this moment in time. The lower than required repeatability should be weighed against the need to design a new calibration unit anyway in case the instrument is to be operated in vacuum. As all blackbodies used are oversized, the reduced repeatability is not seen as a serious constraint for this stage of the project. The final alignment of the detector behind the camera has not yet been performed because it was felt that a slight defocus would not have dramatic effects on the NETD to be measured. Therefore, in order to find the largest noise contributors and possible large deviations, we decided to do a set of preliminary NETD measurements.

### 3.2 NETD Measurements

Until now, the NETD measurements have proven to be more difficult than the optical alignment. The first images produced gave us the confirmation that the optical curvature correction seems to be working, (Fig. 6) but the measured NETD was about a factor of two above the expected NETD and the camera was mounted in a fashion that caused all the data to be in the same column.

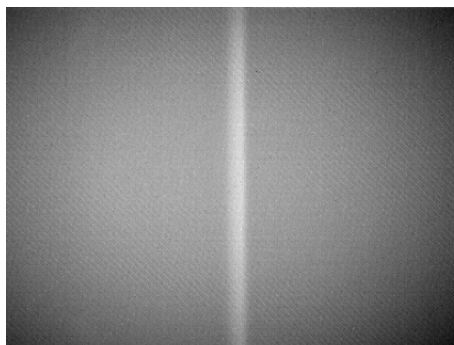


**Fig. 6** Picture showing slit signature at first light

In order to mitigate some of the column effects noticed during the first measurements the camera was rotated so as to allow reference measurements to be taken in

each column, and a calibration sequence was used, with a cold flat plate blackbody to calibrate gain and offset. The gain and offset uses a cold flat plate blackbody (at room temperature) and another hot plate blackbody (at approximately 60 degrees. (it should be noted that this will decrease the measured NETD due to the low effective emissivity of the blackbody (approx 0.9) with about 10%)

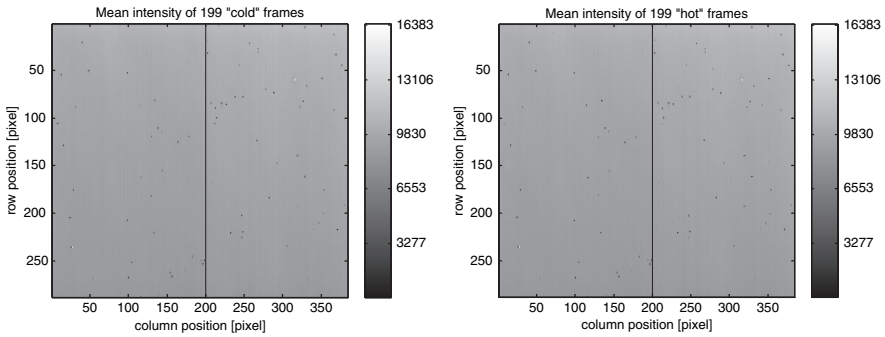


**Fig. 7** Temporal average of 199 frames of “cold” and “hot” target

As can be seen in Fig. 7 there seem to be a number of pixels that give significant differences as compared to the rest. Some bright pixels can be discerned as well as some dark pixels showing less than average signal levels but no signal is visible in the raw image. (the line in the picture indicates the selected line used for further data evaluation)

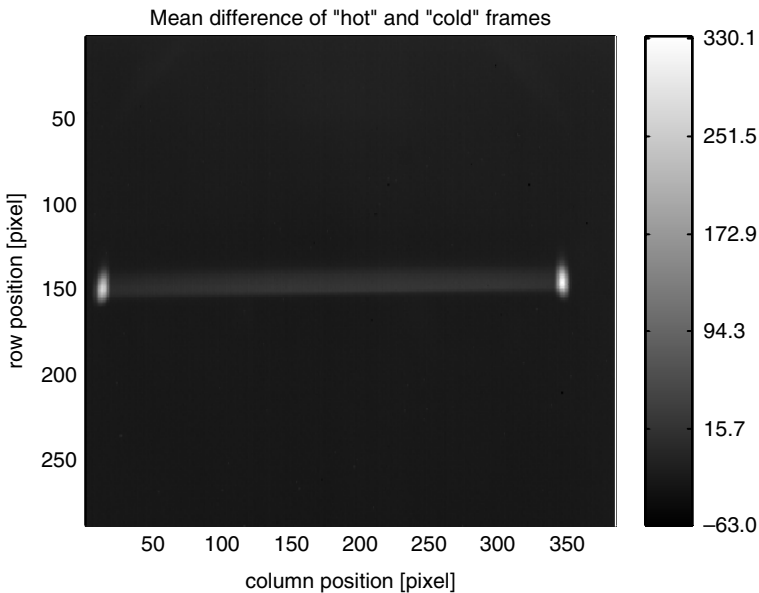


**Fig. 8** Difference of time averaged “hot” and “cold” frames

The signal becomes visible only after correction of gain and offset. Nevertheless the slit image at the detector can be clearly seen as well as the image of the two starting and endpoints of the slit. (The bright spots left and right in the image are caused by drilled holes at the beginning and end of the slit used for the spark erosion manufacturing process.

In order to do some NETD measurements, one column was selected for further analysis. (Fig. 9) which shows that a measurable signal is present.

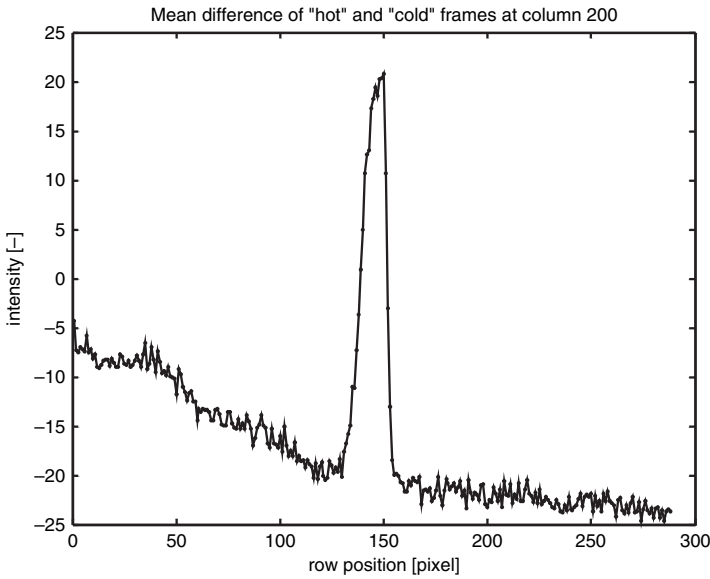


**Fig. 9** Difference of 199 time averaged “hot” and “cold” frames at pixel column 200

The signal has a pulse shaped response with a significantly steeper trailing than leading edge. This is in line with expectations and can be explained when looking at the response of the microbolometer detector. The leading edge is determined by the long wavelength response which gradually improves with decreasing Germanium absorption. (Longer wavelengths are to the left) Shorter wavelengths will be transmitted by the high pass filter deposited on the detector window, and a combination of filter damping and decreased bolometer response cause the response to decrease fast with wavelength.

### ***3.3 Lower than expected NETD and way forward***

As mentioned before, the measured NETD is currently about a factor 2 higher than expected. This prompted some investigations aimed at providing additional insight into the cause of the lower than expected NETD.

During these investigations a number of contributors have been identified. Although the investigations have not been exhaustive a good feeling has been developed regarding the optical throughput of the system.

First of all the reflection of a spare mirror that was coated at the same time as the mirrors used in the breadboard was measured. The results of these measurements showed the reflection to be less than presumed during the NETD calculations. The average reflection at the wavelengths of interest proved to be only 96% whilst 98.5% was anticipated. In first instance this may not seem to dramatic, but considering that the beam passes 7 surfaces, the total system transmission is 0.75 in stead of 0.90 which is more than 16% less.

Furthermore during the initial measurements it was found that the intensity variations of the entire image are quite significant. When tracking the average intensity of the image over time, it can be seen (Fig. 10) that the variation is in the order of 16 AD counts and drift is 8 AD counts. As compared to the signal found in Fig. 9 (40 AD counts) this is considered very significant. Preliminary calculations have shown that this effect has reduced the measured NETD by approximately 35%.

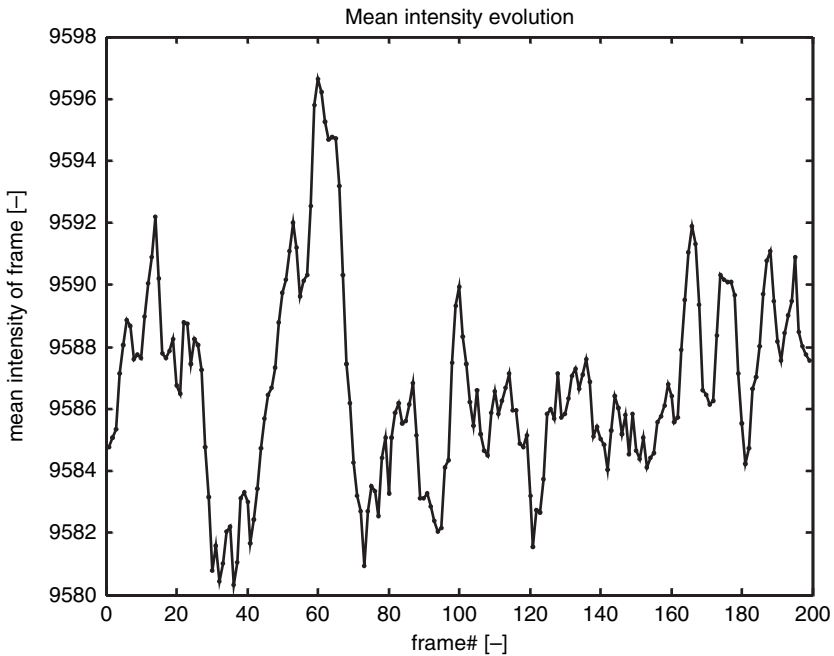


**Fig. 10** Changes in average level over time

The drift shown is more or less expected and is related to the temperature control of the detector and optical bench. The large fluctuations however were not directly expected but may be related to some limit cycling in the thermal control hardware. For normal imaging applications this will not be a real problem, but this becomes a significant effect for the spectrometer application where the input signal is reduced



due to the fact that the available signal is dispersed over a number of pixels. It is not expected that this effect can be easily remedied for the breadboard, as it would involve interference with the thermal control hardware of the camera used.

Another significant contribution to the lower measured NETD is the EMC problems that are currently experienced. Most probably due to a parasitic groundloop, the image is disturbed by a moiré pattern. (Fig. 11) This pattern disturbs the measurements and should be accounted for during the NETD measurements.

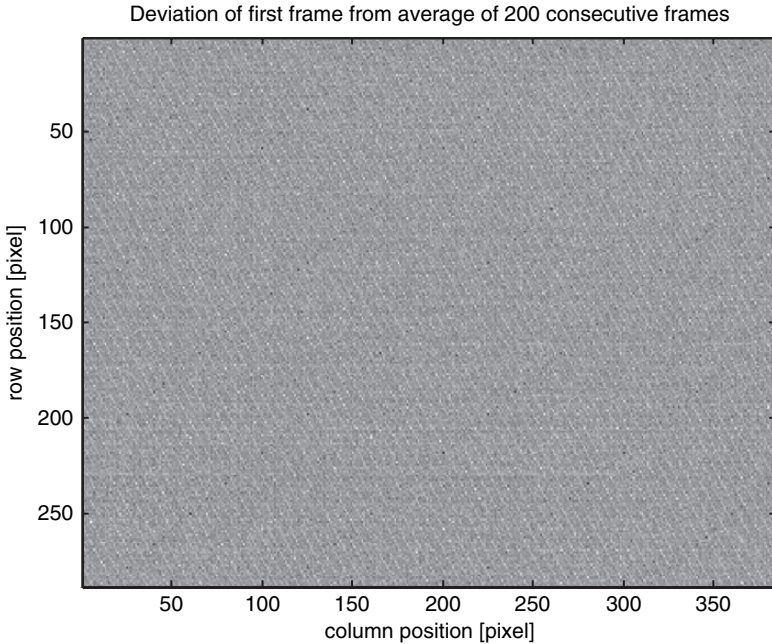
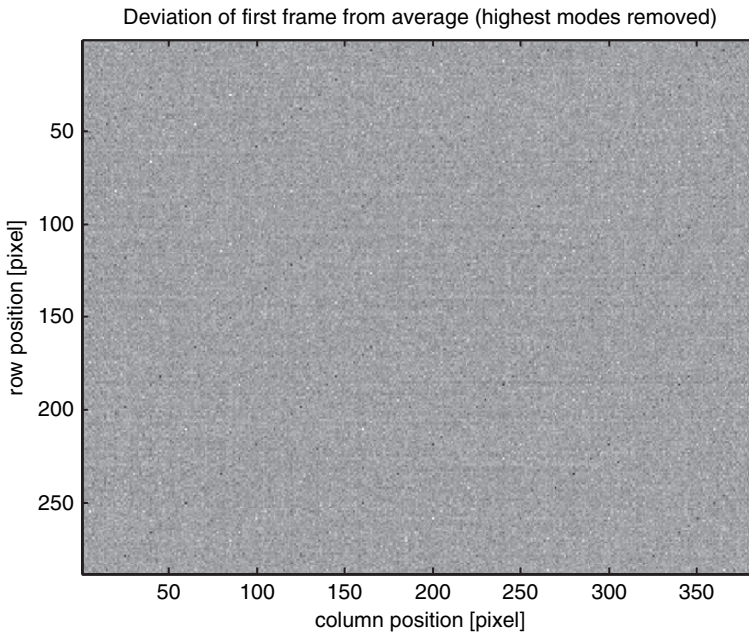


Fig. 11 Deviation of first “cold” frame from time-averaged mean

In order to estimate the obtainable performance without this interference, a 2D FFT of the images was taken and the higher order components removed. This leads to a considerably improved image quality (Fig. 12) and NETD calculated with this improved average where improved by 30% (although some artefacts still exist).

The performed exercises show that the measured NETD is above the expected NETD, but a number of contributors have been identified:

- Poor quality of the blackbody used
- Lower than expected reflection of mirrors
- High average image intensity variations
- EMC disturbance



**Fig. 12** Deviation of first “cold” frame from time-averaged mean with spatial harmonic interference removed (43 modes with highest amplitude in 2D FFT)

## 4 Conclusions

Given the actual situation of the spectrometer as described above and their estimated or calculated influence on NETD it has been concluded that the original NETD calculations will be in line with the measurements results once the above issues are solved. Furthermore a number of potentially relevant issues have not been specifically investigated yet.

- Absorption in the Germanium lenses of the camera
- Effects of defocus on NETD

Furthermore until now the TNO approach of designing an instrument that can be assembled for the majority based on manufacturing tolerances (largely decreasing costs for assembly and alignment) has proven to be working for as far as measurements have been performed. This will lead to an instrument that can be manufactured and aligned at a competitive price. During this year TNO will continue with the characterization of the MIBS breadboard and further results can be expected in the course of this year.